

# Real-Time False-Contours Removal for Inverse Tone Mapped HDR Content

Gonzalo Luzardo  
imec-IPI-UGent  
Ghent University  
Ghent, Belgium  
ESPOL Polytechnic University,  
Escuela Superior Politécnica del  
Litoral, ESPOL  
Facultad de Ingeniería en Electricidad  
y Computación  
Guayaquil, Ecuador  
GonzaloRaimundo.  
LuzardoMorocho@UGent.be

Wilfried Philips  
imec-IPI-UGent  
Ghent University  
Ghent, Belgium  
Wilfried.Philips@UGent.be

Jan Aelterman  
imec-IPI-UGent  
Ghent University  
Ghent, Belgium  
Jan.Aelterman@UGent.be

Hiep Luong  
imec-IPI-UGent  
Ghent University  
Ghent, Belgium  
Hiep.Luong@UGent.be

Daniel Ochoa  
ESPOL Polytechnic University,  
Escuela Superior Politécnica del  
Litoral, ESPOL  
Facultad de Ingeniería en Electricidad  
y Computación  
Guayaquil, Ecuador  
dochoa@fiec.espol.edu.ec

## ABSTRACT

High Dynamic Ranges (HDR) displays can show images with higher color contrast levels and peak luminosities than the commonly used Low Dynamic Range (LDR) displays. Although HDR displays are still expensive, they are reaching the consumer market in the coming years. Unfortunately, most video content is recorded and/or graded in LDR format. Typically, dynamic range expansion by using an Inverse Tone Mapped Operator (iTMO) is required to show LDR content in HDR displays. The most common type of artifact derived from dynamic range expansion is false contouring, which negatively affects the overall image quality. In this paper, we propose a new fast iterative false-contour removal method for inverse tone mapped HDR content. We consider the false-contour removal as a signal reconstruction problem, and we solve it using an iterative Projection Onto Convex Sets (POCS) minimization algorithm. Unlike most other false-contour removal techniques, we define reconstruction constraints taking into account the iTMO used. Experimental results demonstrate the effectiveness of the proposed method to remove false contours while preserving details in the image. In order speed up the execution time, the proposed method was implemented

---

Permission to make digital or hard copies of all or part of this work for personal or classroom use is granted without fee provided that copies are not made or distributed for profit or commercial advantage and that copies bear this notice and the full citation on the first page. Copyrights for components of this work owned by others than the author(s) must be honored. Abstracting with credit is permitted. To copy otherwise, or republish, to post on servers or to redistribute to lists, requires prior specific permission and/or a fee. Request permissions from permissions@acm.org.

MM'17, October 23–27, 2017, Mountain View, CA, USA.

© 2017 Copyright held by the owner/author(s). Publication rights licensed to ACM.  
ACM ISBN 978-1-4503-4906-2/17/10...\$15.00  
<https://doi.org/10.1145/3123266.3123400>

to run on a GPU. We were able to show that it can be used to remove false contours in real-time from an inverse tone mapped High-definition HDR video sequences at 24 fps.

## 1 INTRODUCTION

Conventional image display and acquisition technologies work on a relatively narrow range of luminosities levels in the order of 7 to 9 stops. Images captured with such devices are called Low Dynamic Range (LDR) images. High Dynamic Range Imaging (HDRI) devices yield images with a larger range of luminosities and therefore better visual impressions than its LDR counterpart [16].

High Dynamic Range (HDR) content encodes dark areas darker and bright areas brighter, these characteristics give an increased sense of detail, sharpness, clarity, color and saturation. Nowadays, HDR prototype displays can show images with high dynamic range that could potentially go up to 20 stops and peak luminosities up to 6000 cd/m<sup>2</sup> (nits) [1]. Likewise, it is expected that HDR displays capable of reproducing HDR content in the order of 12 to 14 stops and luminance ranges between 1000 and 4000 nits, will reach the consumer market at reasonable prices in the coming years. These developments will certainly improve the visual experience of watching movies and playing games.

Unfortunately, most video content is recorded and/or graded in LDR. To display LDR images on an HDR display, a LDR-to-HDR conversion step called Inverse Tone Mapping Operator (iTMO) is required. iTMOs usually begin with the linearization of the original LDR image values to their corresponding real-world radiance values. Then, intensity values are expanded to increase the image's dynamic range and bit-depth. In practice, only high intensity values are

expanded, low values are compressed and the mid values remain unchanged [4, 19].

LDR content expansion can create and emphasize image artifacts known as false contours that degrade the overall image quality. They often appear in texture-less regions containing smooth gradients. An example of a quantized HDR image is shown the Figure 1. The unnatural appearance of discrete color bands is caused by the coarse quantization of the sky region into finite codewords, a larger number of codewords is needed to obtain a gradual color transition [13]. Moreover, well-known image processing techniques such as contrast enhancement or histogram-based manipulation, tend to make false contours even more pronounced.



**Figure 1: Original image (left) and quantized image (right).**

To deal with false contours, two common approaches are: 1) False-contours prevention: to prevent the generation of visible false-contours during expansion [3, 10] and 2) False-contour removal: to reduce the visibility of false contours generated by expansion [6, 9, 11, 17, 18, 20, 23]. In this paper, we propose a new iterative false-contour removal method based on the theory of Projection Onto Convex Sets (POCS) [7, 8]. The proposed method tackles the problem of real-time de-quantization of inverse tone mapped HDR image sequences. Our technique combines real-time processing with robust artifact suppression. Real-time processing is achieved via GPU acceleration by exploiting the Quasar programming language [12]. Robust artifact suppression is done by using prior knowledge of the intensity levels values of quantization edges in the inverse tone mapped HDR image by means of the operator used for the expansion procedure.

This paper is organized as follows: An overview of previous works is given in Section 2. Then, the formulation of the false-contour problem and the description of the proposed method are described in Section 3. Experimental results are presented in Section 4. Finally, concluding remarks are discussed in Section 5.

## 2 PREVIOUS WORK

Several methods to remove false-contour artifacts in images after its expansion to a higher bit-depth have been proposed. Daly [9] describes a de-contouring method for noisy images based on an adaptive coring function. In this approach, a higher N-bit-depth version of the original image is filtered using a sieve filter, a modified version of the bilateral filter [21], to smooth contours and preserve sharp edges of the original image. Then, the filtered image is subtracted from the original image to obtain a so-called high-pass (HP) component. At this stage, only contour artifacts related to low spatial frequency are extracted. To remove high-frequency false-contours, an adaptive coring function to reduce low intensity

values in the HP component is applied. A coring function acts as a non-linear filter on each pixel of HP. Pixel values smaller than a threshold  $b$  are attenuated, otherwise they are left unchanged [5]. The threshold  $b$  is modified according to the local spatial activity in order to remove the contours located at regions with smooth gradients, more activity meaning less coring and vice versa. The author explored two types of measurement of local activity: standard deviation and sum of absolute differences. Finally, the de-contoured image is computed by adding the result of the adaptive coring function with the original higher N-bit-depth version of the image. This method is more effective than the previous method proposed by the author [11], however it can lead to removal of useful signals that cannot be distinguished from contouring. Also, the use of the sieve filter makes it computationally demanding.

Bhagavathy et al. [6] describe a method to suppress contour artifacts using multi-scale probabilistic dithering. First, a multi-scale analysis of the color distribution in the neighborhood of each pixel is done to determine the presence and scale of contour artifacts. Later, these contours are made less visible to the human eye using probabilistic dithering. This method is effective to hide contour artifacts at different scales with preservation of small details at flat regions, however multi-scale analysis takes many calculations.

A simple but effective method is presented by Xu and Kim [23]. Their approach consists in three steps. First, for each pixel, a directional segmentation (at eight different orientations) using a 3x15 rectangular window is performed to find out a local support region, which contains only slowly changing luminance (smaller than a predefined quantization level). Pixels that lie on an object edge will have a small local support region in contrast with those pixels within a false contour. Afterwards, the resulting support region is evaluated to determine if it corresponds to a smooth area or one with small magnitude details. The total number of zero-crossings of the luminance gradient is used to approximate the amount of high-frequency content within the support region. Less high-frequency content, the more likely that this support region is from a smooth area. This value is used to apply a low-pass filter on the support region that is tailored to the amount of high-frequency detected, high-frequency content leads to less smoothing. Finally, a spatial dithering method with a 4x4 dithering mask is applied to the image to prevent new contours due to the low-pass filter. The proposed method reduces contour artifacts while keeping the small details intact. In addition, authors successfully tested an implementation of their algorithm running on a FPGA chip.

In recent studies, Mizuno and Ikebe [17] propose a false-contour removal method which considers the inherent noise of natural images. This approach takes into account that the original analog signal fluctuates due to noise before quantization. Therefore, they define a quantization formulation that includes such noise. The de-contoured image is obtained by Maximum-A-Posteriori (MAP) estimation aimed at finding the most probable de-contoured high bit-depth image based on the original one with false contours. Wan et al. [22] propose a method to remove false contours based on the formulation of an optimization problem that minimizes the average mean squared error (MSE) between the original high bit-depth image and the de-contoured smoothed version. The optimization is solved using a two-step approximation strategy: first the AC component is estimated using MAP, then distortion-minimizing

high bit-depth DC component is computed by minimizing the MSE. These two approaches provided good false-contours removal, both in artificial and natural noisy images, but they may be computationally intensive. In optimization-based approaches, complexity depends not only on the image's size, but also on the parameters selection and the amount of contours to be removed.

Song et al. [20] propose a de-banding method for inverse tone mapped HDR images based on a selective 1D sparse filter. This method not only removes false contours but also other artifacts. A sparse 1D filter is selectively applied only in smooth regions of the image where banding is usually observed, therefore details in the original image are preserved. Smooth region detection and filtering are performed simultaneously in a 1D sparse region of the image. The detection is done using adaptive thresholding on the absolute value of the differences between the central pixel and its sparse neighbors. Since the codewords of the corresponding pixels of the banding areas at the LDR image are very similar to each other, but after the inverse tone mapping these difference increases, the threshold is computed in each segment by taking into account the iTMO used during the conversion. The visual evaluation of this method was performed using a Dolby Pulsar HDR screen. Results of the study showed that it can visible remove false contours in HDR images. According to the authors, due to its simplicity and low use of memory, this method can easily be implemented in hardware.

In this paper, we propose a new fast iterative false-contour removal method for Inverse Tone Mapped HDR content. Our method considers that false-contour removal operation can be seen as a signal reconstruction problem that can be solved using an interactive POCS based minimization algorithm. As in [20] we define some constraints taking into account the iTMO used during the conversion as well as the specific characteristics of quantization edges in the inverse tone mapped HDR content.

### 3 PROPOSED METHOD

Most de-banding methods mainly focus on removing false contours on HDR images without any clue about how these false contours were created by the dynamic range expansion of the original LDR image. These methods involve a false-contour detection step, these contours are removed in subsequent steps. Detection approaches do not consider that all contours edges in the image have different contrast due to the non-linear expansion operator used by the iTMO. Hence, image details may be regarded as false contours or even some false contours could be not recognized at all. Our method exploits the non-linear change in contrast of LDR image edges at smooth gradient regions in the HDR domain due to the expansion operator used by the iTMO. In this way, false contours will be detected, regardless of whether smooth regions have different contrasts in the expanded HDR image.

#### 3.1 Problem formulation

False-contour removal is basically a problem of signal reconstruction. Let  $\vec{w}_l$  be the LDR image input of dimension  $M \times N$  reshaped as a vector of  $MN$  rows, we can write the inverse tone mapped, expanded version of it (with banding artifacts), as:

$$\vec{w} = f(\vec{w}_l)$$

With  $f(\cdot)$  a monotonic function performing pixel-wise expansion to the HDR luminance range. Then the signal reconstruction problem can be formulated as:

$$\hat{\vec{y}} = \arg \min \|H\vec{y}\|^2 \quad \text{s.t.} \quad \|f^{-1}(\vec{w}) - f^{-1}(\vec{y})\|_\infty \leq q \quad (1)$$

With  $f^{-1}(\cdot)$  the inverse function of  $f(\cdot)$  and  $q \in \mathbb{R}_+$  where

$$\|\vec{x}\|_\infty = \max_{i \in [0..N]} |\vec{x}_i|$$

Where  $\vec{y}$  is the solution vector of  $MN$  rows (image without false contours) and  $H$  is a square matrix with a dimension of  $MN \times MN$  that represents a high-pass filter. The matrix  $H$  allows to penalize the solution with a large amount of high frequencies (high amount of banding/false-contours). In this way, we reward those solutions with smooth changes in intensity values (without false contours).

The constraint in (1) is based on the fact that quantization edges in  $\vec{w}$  differ from other edges because the first ones have only a small difference of one intensity value in the corresponding LDR image  $\vec{w}_l$ . Hence,  $q$  represents this small difference between two consecutive pixels in a smooth region in  $\vec{w}_l$  that generates false contours in  $\vec{w}$ .

#### 3.2 False-contour removal based on POCS algorithm

The problem in (1) can be solved using an iterative POCS based minimization algorithm [7, 8]. The constraint  $\|\cdot\|_\infty \leq q$  corresponds to a hypercube around  $\vec{x}$  with sides  $2q$ , note that all points within the hypercube constitute a convex set. The expansion tone mapping function  $f(\cdot)$  transforms the cube into a cuboid shape with respect to  $\vec{y}$ , which is still a convex set. A simple projection operator onto this set is given by:

$$\mathcal{P}_Q(\vec{y}) = \begin{cases} f(w_{l,i} - q) & y_i < f(w_{l,i} - q) \\ y_i & f(w_{l,i} - q) \leq y_i \leq f(w_{l,i} + q) \\ f(w_{l,i} + q) & f(w_{l,i} + q) < y_i \end{cases}$$

Additionally, it can be shown that one step of gradient descent w.r.t. the cost function  $\|H\vec{y}\|^2$ , corresponds to a projection onto a hypersphere around  $\vec{0}$  w.r.t. the constraint  $\|\vec{y}\|^2 \leq b$  using a certain constant  $b \in \mathbb{R}_+$ . Note that the set of all points within the hypersphere also form convex set:

$$\mathcal{P}_B(\vec{y}) = (1 - \epsilon H^T H) \vec{y}_j$$

Therefore, following the theory of POCS, the optimum of (1) can be found by allowing iterative convergence of the cascaded projection operators:

$$\vec{y}_{j+1} = \mathcal{P}_Q(\mathcal{P}_B(\vec{y}_j))$$

The matrix  $H$  can be interpreted as a high-pass filter based on subtraction of the consecutive pixels-values. In this way, the operator  $\mathcal{P}_B$  can be seen as a low-pass filter based on the average of

consecutive pixels. A graphic representation of the proposed iterative method is shown in Figure 2. In the first part of iteration, the image is low-pass filtered (projected to  $\mathcal{S}_B$ ) using  $\mathcal{P}_B$ . Then, the result is clipped (projected to  $\mathcal{S}_Q$ ) using  $\mathcal{P}_Q$ , which considers the constraint related to the bounds imposed by  $q$  in the LDR domain.

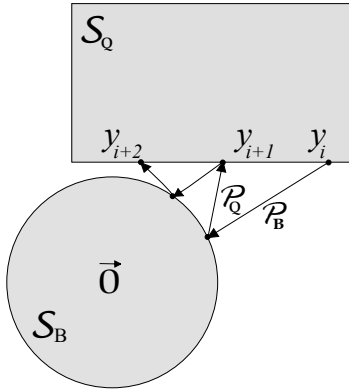


**Figure 2: Graphical representation of the proposed iterative POCS algorithm.**

### 3.3 Implementation using Quasar Framework

The Quasar framework consists of a compiler system, a runtime library and an IDE. The developer uses a set of common high-level programming structures and libraries for coding. Then, the framework automatically detects and extracts serial and parallel loops in the code that can be executed on the specific GPU, by allowing speed-up the execution time of the program. This way, the programmer is relieved from complicated implementation issues relating to GPGPU (General-purpose computing on graphics processing units) programming and can focus on the specification and improvement of the algorithms [12].

The proposed method was implemented using Quasar framework in order to exploit the compute power of the GPU in all pixel-per-pixel operations. Also, we used a variety of optimization techniques recommended in Quasar documentation to ensure the best run-time execution. As a result, the execution time of the proposed method is 600 times faster than the same implementation in a program language that uses the native CPU support for process execution.

## 4 EXPERIMENTAL RESULTS

We compare the proposed false-contour removal method (POCS) with "De-contouring via multi-band coring" proposed by Daly [9] and "De-banding and visual enhancement filter" proposed by Song et al. [20], which we consider to be the most promising approaches for real-time execution. Both methods were implemented in Quasar and executed using the default parameters suggested by the authors. We decided to implement these methods in Quasar in order to make a fair comparison with our POCS method.

Figure 3(a) shows an inverse tone mapped synthetic HDR image with false contours as a result of the expansion operation by Kovaleski and Oliveira [14] iTMO to bring them to SIM2 HDR47ES6MB display characteristics (6000 nits peak brightness, sRGB color space,

1920x1080 resolution and 16 f/stops contrast) [1]. The original synthetic LDR image has a wide smooth gradient from the left to right of the image. The six white dots represent small details which need to be preserved after the de-contouring procedure.

Results in Figure 3 show that our proposed POCS method (d) can reduce false contours while preserving details (white dots) as well as Song et al. method (c). However, we can observe that Daly(d) was unable to remove false contours from (a). These results were validated by simple observation on the SIM2 display and we got the same findings.

To compare effectiveness of the proposed method, two 1-D intensity profiles along the highlighted segments (40 pixels) from Figure 4(a) were extracted. As shown in Figure 4(b) and Figure 4(c), all methods preserve the details (dots) in the original image. However, the proposed POCS method shows the best results in reducing false contours, showing a smoother curve compare with the other approaches.

Similarly, we tested our method using non-synthetic HD LDR video sequences available in Xiph.org Video Test Media (derf's collection) [2]. In this article, we show the results obtained from videos "Elephants dream" and "Sintel trailer", because for both, a large amount of false contours appears when they are inverse tone mapped by Kovaleski and Oliveira iTMO to bring them to SIM2

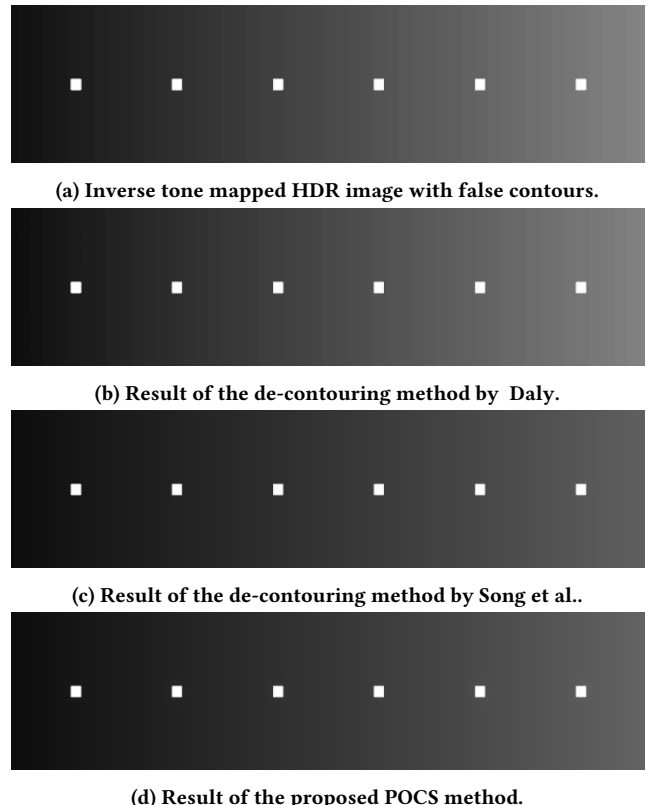


**Figure 3: Results of the proposed method on a synthetic image. HDR images were tone mapped by Mantiuk et al. [15] operator. These images are best viewed in the electronic PDF version.**

display characteristics. Table 1 shows examples of the results of this test, two from each video sequence. The region with the most evident false-contours are zoomed-in to better observe the contour reduction effect of each method. As can be seen in Table 1, the proposed POCS method shows the best results in reducing false contours.

For synthetic and non-synthetic images, we fixed the maximum number of iterations to 10. However, we found that in most of cases,

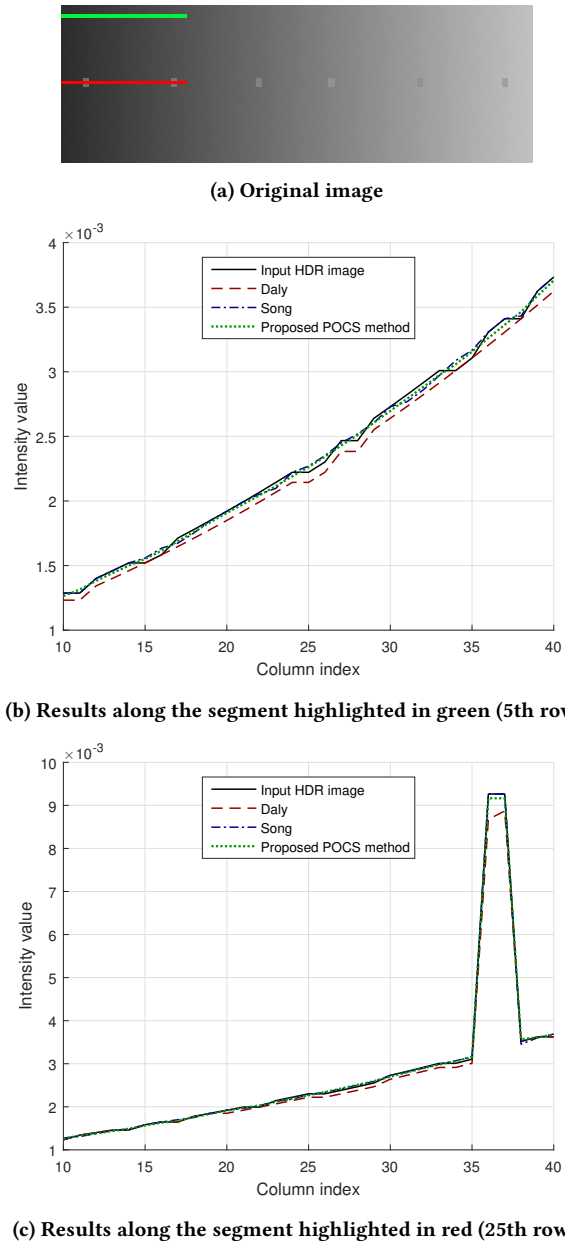


**Figure 4: Comparison between the proposed POCS method and other approaches by Song et al. and Daly, on 1-D intensity profile along a highlighted line segments marked in (a).**

the algorithm converges to a good solution, this means without noticeable false-contours, in the seventh iteration. Likewise, for synthetic and non-synthetic images we found that we got the best results by fixing the radius of the low-pass filter to 3 and 7, respectively. Despite these findings, a more detailed analysis on the radius of the low-pass filter and the number of iterations is required before the algorithm converges, was conducted.

POCS theory ensures that as the number of iterations tends to infinity, the solution converges to the global optimum restricted to the constraints. In our approach, the convergence rate depends on to radius of the low-pass filter: each iteration expands the support of the resulting kernel with roughly twice the radius. The size of the image is a lower limit for the resultant kernel support. So, the larger the kernel size, the fewer iterations are required to reach convergence. Therefore, two important questions arise: which is the best radius value for the low-pass filter in our method? and how it is related with the convergence rate?

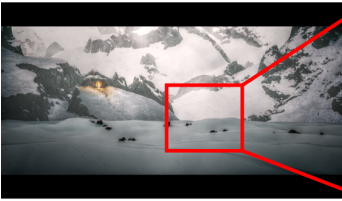
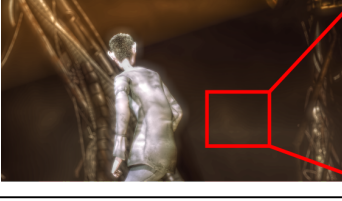
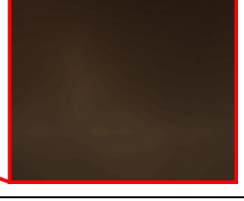
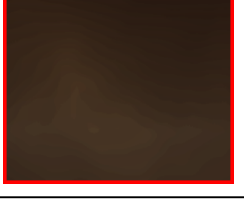
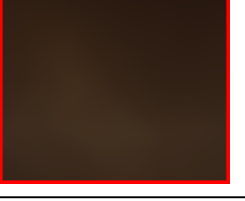
In order to answer these questions, we carried out an experiment to check the convergence of our algorithm in typical conditions using all the frames from the sequences "Sintel trailer" and "Elephant dreams". We tested the convergence with the following radius values for the low-pass filter: 1, 3, 5, 7, 9, 11, 13 and 15. Typical convergence graphs were obtained of this study, one per frame, where the x-coordinate represents the number of iteration and y-coordinate represents the distance (Root-Mean-Square Distance) between the current image and the image in the last iteration (until it converges with a maximum of 1000 iterations). Note that we got eight different images in the last iteration (8 different global solutions), one per each radius value.

A global graph of convergence was computed by averaging the y-values for all graphs obtained in both video sequences, see Figure 5(a). Eight different curves were obtained, one for each radius value. When visually analyzing the output image in each iteration at the SIM2 HDR display, we realized that a good solution without noticeable false-contours is reached when the distance between the image in the current iteration and the image in the last iteration is less than 0.5. From Figure 5, we found that our algorithm converges to a good solution (red line in the graph) at the 58th, 13th, 7th and 5th iteration for a radius equal to 1, 3, 5 and 7, respectively; and at the 4th iteration for a radius equal to 9, 11, 13 and 15, see Figure 5(b). In addition, as might be expected, we found that increasing the radius lead to faster convergence-speed, however this could be decrease the overall image contrast.

To analyze the computation-time as a function of the radius of the low-pass filter the average computation-time for different radius values were computed, see Figure 6. In this graph, the x-coordinate represents the radius and the y-coordinate represents the average computation-time in milliseconds until the algorithm converges to a good solution. Each point in the graph shows the average number of iterations that were required for convergence. We found, as might be expected, that the computation-time lead to decrease with the increasing of the size of the radius. Additionally, we found that the best radius values to use are 7 (19.55 ms) and 11 (18.34 ms) with an average number of iterations until convergence of 4 and 3, respectively.

Taking into account these results, we can conclude that, using a radius of 7 and a maximum number of iterations of 4, our method

**Table 1: Examples of the results obtained in the test with non-synthetic LDR video sequences. The region with the most evident false-contours (red square) are zoomed-in. HDR images were tone mapped by Mantiuk et al. [15] operator. These images are best viewed in the electronic PDF version.**

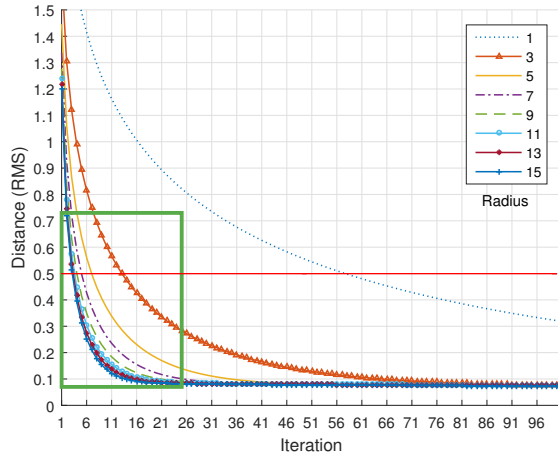
Original HDR image tone mapped by Mantiuk et al. [15] operator.	Results.		
	Daly	Song et al.	Proposed method
			
			
			
			

can tackle the problem of real-time de-contouring of a HD-HDR video sequence at 24 fps. Note that the maximum computing-time to process one frame of a HD video in real-time at 24 fps is 41.66 ms. Despite this, a last experiment was carried on to compare the computation-time to process one video frame using the proposed method versus those obtained with the methods proposed by Daly [9] and Song et al. [20]. For this, we only use the entire video sequence of "Sintel trailer" for testing. The parameters used for radius and maximum number of iterations were 7 and 4, respectively. Table 2 shows the results of this test. As expected, Daly method is the slowest of all because it incorporates a time-consuming edge preserving filter (sieve filter). Also, taking into account the maximum computation-time (Max column), clearly both Song et al. and our POCS method can remove false contours on HDR-HD video sequences at 24 fps.

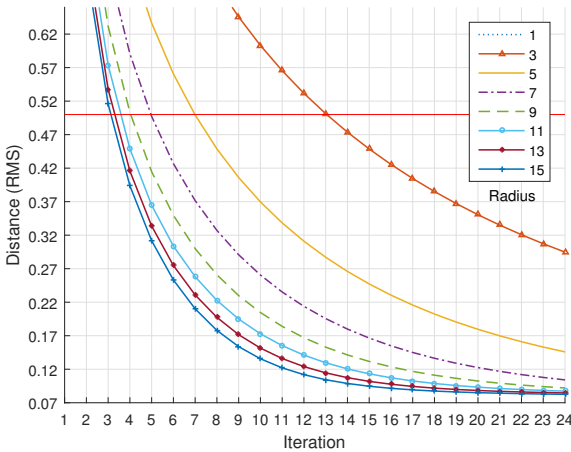
All results showed in this article can be downloaded in EXR format and its correspondent tone mapped version in PNG format from <https://telin.ugent.be/~gluzardo/pocs.html>

**Table 2: Computation-time to remove false contours at one HD video frame in milliseconds (ms)**

Method	Avg.	Min.	Max.
Daly	102.04	94.03	253.02
Song et al.	9.99	4.04	17.12
POCS	19.67	13.78	20.21



(a) Global Convergence Graph until the 100th iteration.



(b) Zoom into the area within the green rectangle.

Figure 5: Global Convergence Graph of the proposed algorithm.

## 5 CONCLUSIONS

We proposed a method to remove false contours in inverse tone mapped HDR content, based on the principle of POCS. Our method is premised on the fact that disturbing quantization edges are most apparent in smooth gradients in the LDR images and these are non-linearly expanded by the iTMO. It is based on projections onto convex sets (POCS), iterating between the convex sets of smooth images and the set of images that would match to the quantized input. Eventually, it converges to a smooth, yet data-accurate image. In doing this, the algorithm distinguishes false edges due to quantization from true edges because intensities related to the latter edges would not quantize the same code values. We tested our method in both synthetic and non-synthetic images and video sequences.

We have provided experimental results demonstrating the effectiveness of the proposed method in reducing the visibility of false contours and preserving small details in the image and its potential

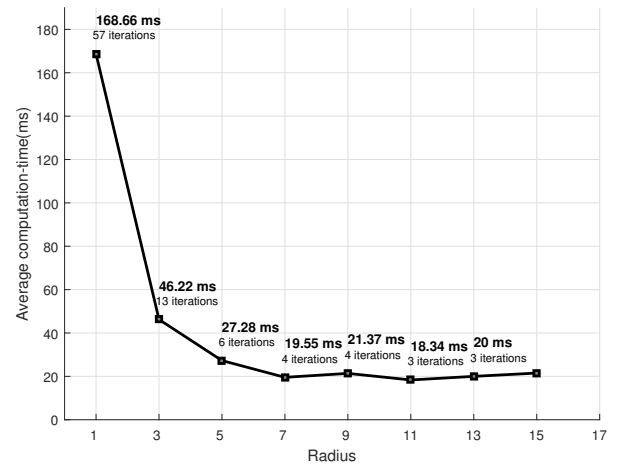


Figure 6: Average computation-time vs. Radius of the low-pass filters.

for real-time processing. Compared to other methods, ours provides better visual perception of smooth gradient regions which is supported by the image profiles extracted from the test data sets.

Our method can also be potentially used for bit-depth enhancement of low bit-depth LDR images. In this case, the expansion operator could be a simple linear function.

A potential disadvantage of the proposed method is the need of knowing the iTMO as a input parameter, however in practice this information is known in advance.

## ACKNOWLEDGMENTS

This work was supported by the imec-HD<sup>2</sup>R project. The work of G. Luzardo was supported by Secretaría de Educación Superior, Ciencia, Tecnología e Innovación (SENYCYT) and Escuela Superior Politécnica del Litoral (ESPOL) under Ph.D. studies 2016. Jan Aelterman is currently supported by Ghent University postdoctoral fellowship (BOF15/PDO/003).

## REFERENCES

- [1] 2017. SIM2 HDR display - HDR47ES6MB. (2017). Retrieved February 21, 2017 from <http://hdr.sim2.it/hdrproducts/hdr47es6mb>
- [2] 2017. Xiph.org Video Test Media [derf's collection]. (2017). Retrieved February 21, 2017 from <https://media.xiph.org/video/derf/>
- [3] Wonseok Ahn and Jae-Seung Kim. 2005. Flat-region detection and false contour removal in the digital TV display. In *Multimedia and Expo, 2005. ICME 2005. IEEE International Conference on*. IEEE, 1338–1341.
- [4] Francesco Banerle, Alessandro Artusi, Kurt Debattista, and Alan Chalmers. 2011. *Advanced high dynamic range imaging: theory and practice*. CRC press.
- [5] Bryce E Bayer and Philip G Powell. 1986. A method for the digital enhancement of unsharp, grainy photographic images. *Advances in Computer Vision and Image Processing* 2 (1986), 31–88.
- [6] Sitaram Bhagavathy, Joan Llach, and Jiefu Zhai. 2009. Multiscale probabilistic dithering for suppressing contour artifacts in digital images. *IEEE Transactions on Image Processing* 18, 9 (2009), 1936–1945.
- [7] LM Breg. 1965. Finding the common point of convex sets by the method of successive projections. *Dokl. Akad. Nauk SSSR* (1965), 487–490.
- [8] G Crombez. 1991. Image recovery by convex combinations of projections. *J. Math. Anal. Appl.* 155, 2 (1991), 413 – 419. [https://doi.org/10.1016/0022-247X\(91\)90010-W](https://doi.org/10.1016/0022-247X(91)90010-W)

- [9] S Daly. 2008. Perceptual mechanisms in balancing the visibility of false contours and true details under bit-depth constraints. *IMQA2008* (2008), 1–11.
- [10] Scott J Daly and Xiaofan Feng. 2003. Bit-depth extension using spatiotemporal micrider based on models of the equivalent input noise of the visual system. In *Electronic Imaging 2003*. International Society for Optics and Photonics, 455–466.
- [11] Scott J Daly and Xiaofan Feng. 2004. Decontouring: Prevention and removal of false contour artifacts. In *Electronic Imaging 2004*. International Society for Optics and Photonics, 130–149.
- [12] Bart Goossens, Jonas De Vylder, Simon Donné, and Wilfried Philips. 2015. Quasar—a new programming framework for real-time image/video processing on GPU and CPU. In *Proceedings of the 9th International Conference on Distributed Smart Cameras*. ACM, 205–206.
- [13] Qin Huang, Hui Yong Kim, Wen-Jiin Tsai, Se Yoon Jeong, Jin Soo Choi, and C-C Jay Kuo. 2016. Understanding and Removal of False Contour in HEVC Compressed Images. *IEEE Transactions on Circuits and Systems for Video Technology* (2016).
- [14] Rafael P Kovaleski and Manuel M Oliveira. 2014. High-quality reverse tone mapping for a wide range of exposures. In *Graphics, Patterns and Images (SIBGRAPI), 2014 27th SIBGRAPI Conference on*. IEEE, 49–56.
- [15] Rafal Mantiuk, Scott Daly, and Louis Kerofsky. 2008. Display adaptive tone mapping. In *ACM Transactions on Graphics (TOG)*, Vol. 27. ACM, 68.
- [16] Belen Masia, Gordon Wetzstein, Piotr Didyk, and Diego Gutierrez. 2013. A survey on computational displays: Pushing the boundaries of optics, computation, and perception. *Computers & Graphics* 37, 8 (2013), 1012–1038.
- [17] Akira Mizuno and Masayuki Ikebe. 2016. Bit-depth expansion for noisy contour reduction in natural images. In *Acoustics, Speech and Signal Processing (ICASSP), 2016 IEEE International Conference on*. IEEE, 1671–1675.
- [18] Min-Ho Park, Ji Won Lee, Rae-Hong Park, and Jae-Seung Kim. 2010. False contour reduction using neural networks and adaptive bi-directional smoothing. *IEEE Transactions on Consumer Electronics* 56, 2 (2010).
- [19] Erik Reinhard, Wolfgang Heidrich, Paul Debevec, Sumanta Pattanaik, Greg Ward, and Karol Myszkowski. 2010. *High dynamic range imaging: acquisition, display, and image-based lighting*. Morgan Kaufmann.
- [20] Qing Song, Guan-Ming Su, and Pamela C Cosman. 2016. Hardware-efficient debanding and visual enhancement filter for inverse tone mapped high dynamic range images and videos. In *Image Processing (ICIP), 2016 IEEE International Conference on*. IEEE, 3299–3303.
- [21] Carlo Tomasi and Roberto Manduchi. 1998. Bilateral filtering for gray and color images. In *Computer Vision, 1998. Sixth International Conference on*. IEEE, 839–846.
- [22] Pengfei Wan, Gene Cheung, Dinei Florencio, Cha Zhang, and Oscar C Au. 2016. Image bit-depth enhancement via maximum a posteriori estimation of ac signal. *IEEE Transactions on Image Processing* 25, 6 (2016), 2896–2909.
- [23] Ning Xu and Yeong-Taeg Kim. 2010. A simple and effective algorithm for false contour reduction in digital television. In *Consumer Electronics (ICCE), 2010 Digest of Technical Papers International Conference on*. IEEE, 231–232.